


Cannabis sativa L. leaf by-products extracts: Chemical composition, antimicrobial and *in silico* study

Taha Balafrej^{1*} , Itto Maroui², Hamza Elhrech³, Souad Skalli¹, Nezha Lebki⁴,
Souad Benaich⁵, Abdelhadi Hbib⁶, Nawal Bouyahyaoui⁷,
Lamiae Amallah⁸, Rachida Hassikou¹

¹ Mohammed V University in Rabat, Faculty of Sciences, Plant and Microbial Biotechnologies, Biodiversity, and Environment Center, Department of Biology, Rabat, Morocco

² Department of Basic Sciences, Research laboratory in oral biology and biotechnology, Faculty of dental medicine, Mohammed V University in Rabat, Rabat 10000, Morocco

³ Laboratory of Human Pathologies Biology, Department of Biology, Faculty of Sciences, Mohammed V University in Rabat, Rabat 10106, Morocco

⁴ Polyvalent Team in R&D, Polydisciplinary Faculty, Sultan Moulay Slimane University, Beni Mellal 23000, Morocco

⁵ University Mohammed V in Rabat, Faculty of Sciences, Physiology and Physiopathology Research Team, Rabat, Morocco

⁶ Department of periodontology, International Faculty of Dental Medicine, College of Health Sciences, International University of Rabat, Sala Al Jadida, 11100, Morocco

⁷ Laboratory of Research Odontological Biomaterials and Nanotechnology, Faculty of Dental Medicine, Mohammed V University in Rabat, Rabat 10000, Morocco

⁸ Department of Biology, Faculty of Sciences of Tetouan, Abdelmalek Essaadi University, Tetouan, Morocco

* Corresponding author's e-mail: taha.balafrej@um5r.ac.ma

ABSTRACT

Aims: This study aimed to evaluate the biological potential of *Cannabis sativa* L. leaf co-products obtained through different extraction methods (sonication, maceration, and decoction), with a particular focus on their antimicrobial properties and chemical composition. **Methodology and Results:** Extracts were prepared using sonication, maceration, and decoction, and their antimicrobial activity was assessed against two pathogenic microorganisms: *Aggregatibacter actinomycetemcomitans* JP2 clone and *Candida albicans*. The sonication extract exhibited the highest antibacterial activity against *A. actinomycetemcomitans*, whereas the maceration extract showed strong antifungal activity against *C. albicans*. All extracts, except the decoction, demonstrated both bactericidal and fungicidal effects. Chemical characterization was performed using High-Performance Liquid Chromatography (HPLC), revealing the presence of cannabinoids (notably cannabidiol and HU-331) along with flavonoids, phenols, alkaloids, and dihydrostilbenoids. Additionally, molecular docking analysis predicted strong interactions between several identified compounds and bacterial target proteins, indicating promising drug-like properties. **Conclusion, Significance and Impact:** These findings suggest that *Cannabis sativa* L. leaf co-products represent a valuable and underutilized source of bioactive compounds with significant antimicrobial potential. This study highlights their relevance for future pharmaceutical applications and supports their valorization within a sustainable biorefinery approach.

Keywords: antibacterial, antifungal, *Cannabis sativa* L., chemical composition, molecular docking.

INTRODUCTION

Since the beginning of human societies, medicinal plants were essential for the treatment of several illness (Jamshidi-Kia *et al.*, 2017). They

are well-known for their diversity of bioactive compounds that have antimicrobial, anticancer, anti-inflammatory, and so on activities (Jamshidi-Kia *et al.*, 2017). *Cannabis sativa* is one of the earliest plants cultivated by humans, historically reported

for a variety of purposes including medicine, textile, cosmetic, and recreational (Bonini *et al.*, 2018). Their therapeutic properties are primarily due to its richness in secondary metabolites, especially cannabinoids, flavonoids, terpenes, and alkaloids (El Mernissi *et al.*, 2024). Indeed, CBD and THC were the most studied compounds in *Cannabis sativa*. Since the discovery of their structure numerous researches have been done around, their benefits for human health (Schrot and John, 2016).

Microorganisms are ubiquitous, they usually interact with humans (Rather *et al.*, 2021). Some of them can be pathogenic and cause microbial infection and death (Rather *et al.*, 2021). In order to struggle these pathogens, medicinal plants were mainly used for a long time until the emergence of the antibiotic development (Abdallah *et al.*, 2023). However, over the course of evolution, microbial pathogens have acquired multiple mechanisms that allow them to withstand the inhibitory and microbicide effects of antimicrobial agents (Varela *et al.*, 2021). The multi-resistant microbes cause socio-economic and health impact. To overcome these troubles, natural products become an important segment of modern medicine as an innovative antibiotic (Kebede *et al.*, 2021).

Among the most clinically relevant pathogens, *Aggregatibacter actinomycetemcomitans* JP2 clone is a Gram-negative bacterium strongly associated with aggressive periodontitis and systemic infections (Gholizadeh *et al.*, 2017), while *Candida albicans* is an opportunistic fungal pathogen responsible for a wide spectrum of infections (Sardi *et al.*, 2010). Both pathogens exhibit increasing resistance to conventional treatments, highlighting an urgent need for novel therapeutic alternatives. Despite the growing interest in *Cannabis sativa* L. as a source of bioactive compounds, most research has focused on flowers and seeds, while leaves particularly those discarded as by-products after mechanical processing remain largely under-explored. This represents a significant scientific gap, as these by-products may retain biologically active secondary metabolites with antimicrobial potential. Furthermore, the influence of extraction methods and solvent polarity on the chemical composition and biological activity of such leaf extracts has not been systematically investigated. *In silico* approaches, which allow the exploration of molecular interactions between bioactive compounds and microbial targets, have rarely been applied to *Cannabis sativa* L. leaf by-product

extracts, leaving the mechanistic basis of their potential antimicrobial activity largely unknown.

To address these gaps, the aim of this study was to evaluate the antimicrobial activity of *Cannabis sativa* L. leaf by-product extracts against *Aggregatibacter actinomycetemcomitans* JP2 clone and *Candida albicans*, and to characterize their chemical composition using HPLC analysis. Additionally, *in silico* molecular docking approaches were employed to explore potential interactions between identified bioactive compounds and selected molecular targets of the tested pathogens.

This study was guided by the following scientific hypotheses:

- H1: *Cannabis sativa* L. leaf by-product extracts exhibit measurable antimicrobial activity against *Aggregatibacter actinomycetemcomitans* JP2 clone and *Candida albicans*.
- H2: The extraction method and solvent polarity significantly influence the chemical composition and, consequently, the antimicrobial efficacy of *Cannabis sativa* L. leaf by-product extracts.
- H3: Bioactive compounds identified in the extracts may contribute to the observed antimicrobial activity and show potential interactions with selected molecular targets, as revealed by *in silico* modelling.

MATERIAL AND METHODS

Preparation of extracts

Dried *Cannabis sativa* L. leaf by-products were ground into a fine powder using a domestic grinder (MCG-151, Mellerware). For each extraction method, 10 g of powder were mixed with 100 mL of solvent (1:10, w/v).

Maceration extraction

The powder was soaked in ethanol (70% v/v) and continuously stirred using a magnetic stirrer (ARE, VELP Scientifica) at speed level 3 (scale 1-10) at room temperature 25 ± 2 °C for 24 h (Figure 1). The mixture was filtered under vacuum using Whatman filter paper grade 1. The filtrate was concentrated using a rotary evaporator (G1, Heidolph) under reduced pressure at 40 °C. The resulting extract was freeze-dried using a lyophilizer (1LPHA 1-2 LD Plus, CHRIST), stored at -20 °C, and protected from light until further use.



Figure 1. Maceration of *Cannabis sativa* L. leaf by-product powder in 70% ethanol under magnetic stirring

Ultrasound-assisted extraction

The powder was mixed with ethanol (70% v/v) and subjected to ultrasound treatment using a sonicator (Elmasonic S 30 H, Elma Schmidbauer, Germany) operating at 37 kHz and 80 W for 45 min at room temperature (Figure 2). The extract was then filtered, concentrated, and lyophilized as described above.

Decoction extraction

The powder was extracted by decoction under reflux in distilled water for 15 min (Figure 3). The mixture was filtered using Whatman paper grade 1 and concentrated at 40 °C using a rotary evaporator. The aqueous extract was freeze-dried and stored under the same conditions.

Microbial strains studied

Antimicrobial activity was evaluated against *Aggregatibacter actinomycetemcomitans* CCUG 56172 (serotype b, JP2 clone) (Figure 4) and *Candida albicans* ATCC 90028 (Figure 5). Strains were obtained from Oral Biology and Biotechnology Research Laboratory at the Faculty of Dental Medicine of Rabat and stored at -80 °C.

Culture and isolation

A. actinomycetemcomitans JP2 clone was cultured on Dentaid 1 (Brain heart infusion agar (CM1136, OXOID) added with 5 g of yeast extract, 1.5 g of sodium fumarate, 1 g of sodium formate, and vancomycin 5 mg/L) as described by Alsina *et al.* (2021) and incubated at 37 °C under 5% CO₂ for 48 h. *C. albicans* was cultured on Sabouraud dextrose agar (CM0041, OXOID) and incubated at 34 °C for 24 h (Odds, 1991). Prior to experiments, strains were subcultured at least

twice. Purity was confirmed by Gram staining and microscopic examination.

In vitro antimicrobial activity

Agar diffusion test (well method)

Microbial suspensions were prepared in distilled water and adjusted to 0.5 McFarland standard using a nephelometre (Sensititre™

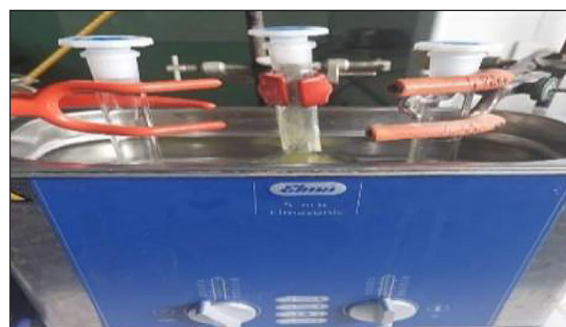


Figure 2. Sonication of *Cannabis sativa* L. leaf by-product powder in 70% ethanol



Figure 3. Decoction of *Cannabis sativa* L. leaf by-product powder in distilled water

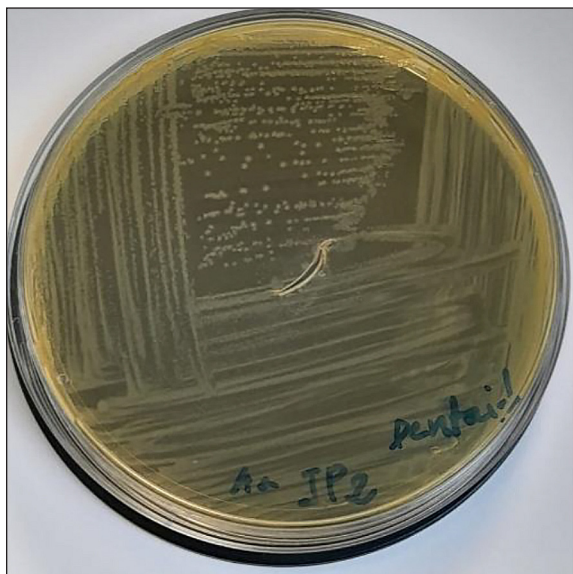


Figure 4. *Aggregatibacter actinomycetemcomitans* CCUG 56172



Figure 5. *Candida albicans* ATCC 90028

Nephelometer, Thermo Fisher Scientific) (Figure 6), corresponding to approximately (around 1×10^8 CFU/mL). The microbial suspension was then spread uniformly by swabbing over the agar surface, with Mueller Hinton agar for bacteria and Sabouraud agar for the yeast, plates with a thickness of 4 mm. Wells of 6 mm diameter were created using sterile Pasteur pipettes. Each well was filled with 60 μ L of extract at 0.1 mg/mL.

Controls included

Positive controls: chlorhexidine (Perio.Aid 0.12%).



Figure 6. Nephelometer used for McFarland standard adjustment

Negative controls: sterile distilled water and hydro-ethanolic solvent (30:70).

Plates were incubated under the conditions described above. Inhibition zones (mm) were measured using a ruler. All experiments were performed in triplicate.

Micro-dilution test

Determination of MIC

MIC values were determined according to Cockerill et Clinical and Laboratory Standards Institute (2012). Extracts were dissolved in hydro-ethanol (3:7) and serially diluted to obtain concentrations ranging from 1–100 μ g/mL].

Each well of a sterile 96-well plate contained: 80 μ L of extract dilution plus 80 μ L of microbial suspension adjusted to 1×10^8 CFU/mL.

Controls:

- Growth control: 80 μ L of distilled water + 80 μ L of the microbial suspension.
- Sterility control: 160 μ L of liquid medium only (BHI or SDI).
- Solvent control: 80 μ L of hydro-ethanolic solution + 80 μ L of the microbial suspension.
- Positive control: 80 μ L of amoxicillin (10 mg/ml) + 80 μ L of the microbial suspension.

Plates were incubated under appropriate conditions. After incubation, 40 μ L of 2% triphenyl tetrazolium (TTC) solution was added, followed by incubation for 3–4 h. MIC was defined as the lowest concentration showing no visible growth and no color change.

MBC and MFC determination

Aliquots (10 μ L) from wells with no visible growth were plated onto agar media and incubated as described. The test was carried out in triplicate.

Colonies were counted, and MBC/MFC was defined as the lowest concentration resulting in $\geq 99.99\%$ reduction in CFU relative to the initial inoculum. The MBC/MIC (or MFC/MIC) ratio is utilized to determine whether the antimicrobial activity of the tested product is bactericidal (or fungicidal) or bacteriostatic (or fungistatic). If the ratio is less than 4, the extracts is classified as bactericidal (or fungicidal); if the ratio is greater than 4, the extracts is classified as bacteriostatic (or fungistatic).

HPLC method

Analysis was performed using a Sciex Exion-LC system coupled to a TripleQuad 3500 mass spectrometer with an APCI source (Thermo Fisher Scientific, Xcalibur software) (Raeber *et al.*, 2024).

Chromatographic conditions

Separation was achieved using a Waters Symmetry C18 column (4.6 × 100 mm, 3.5 μm) maintained at 45 °C. A UHPLC polar C18 pre-column (2.1 mm internal diameter) was installed upstream of the analytical column to protect and extend its lifetime. The injection volume was 5 μL. The flow rate was maintained between 0.6 and 0.7 mL/min throughout the run.

Mobile phases

- Phase A: 2 mM ammonium acetate with 0.1% formic acid in water.
- Phase B: 2 mM ammonium acetate with 0.1% formic acid in methanol containing 5% water.

Gradient program

The chromatographic separation started at 70% B for the first minute. The flow rate was then adjusted to 0.6 mL/min, while the proportion of solvent B was gradually increased to 98% at 20 minutes. This condition was maintained until 26.5 minutes. The system was then rapidly returned to 70% B and re-equilibrated until 28 minutes.

Mass spectrometry conditions

Ionization was performed in positive APCI mode. The source parameters were as follows:

- Scan range (m/z): MS1, 100/1500.
- Curtain gas: 20 psi.
- Collision gas: 9 psi.
- Nebulizer current: 5 μA.
- Source temperature: 500 °C.

- GS1 (nebulizing gas): 45 psi.
- Entrance potential: 10 V.

Data acquisition and processing were performed using Xcalibur software (Thermo Fisher Scientific). Compound identification was based on comparison with reference standards and/or available databases.

Drug likeness

We used the SWISS-ADME online platform (<http://www.swissadme.ch/>) accessed on March 10, 2025, a widely used and reliable tool for predicting pharmacokinetic properties to investigate drug-likeness. SWISS-ADME evaluates several key parameters related to oral bioavailability based on Lipinski's Rule of Five, containing molecular weight (MW), lipophilicity (LogP), and the numbers of hydrogen bond acceptors (nHA) and donors (nHD) (Lipinski *et al.*, 2012).

Molecular docking

Docking simulations were performed using AutoDock Vina v1.1.2 was used to study how the compounds interact with proteins. All the compounds were downloaded from PubCem (<https://pubchem.ncbi.nlm.nih.gov>). The 3D structure files (.sdf) was visualized using PyMol (version 4.6.0) and save in.pdb format. Since the crystal structure of leukotoxin A (Ltx A) isn't available in any protein database, we downloaded its predicted structure from AlphaFold using its UniProt code (P16462), average pLDDT is 72.12 (High). Whereas peptidyl arginine deiminase 4 (PAD4) structure was downloaded from Protein Data Bank (<https://rscb.org>) with the PDB code ID 1WD8. The docking grid dimensions were set to (104Å × 44Å × 40Å) and (46Å × 32Å × 32Å), respectively. Finally, we utilized Discovery Studio 2024 (BIOVIA) for the analyses of the best binding models, and create 2D images of the ligand-protein interaction.

In-silico pharmacokinetic (ADME) analysis

To predict how the compounds are absorbed, distributed, metabolized, excreted, and how toxic they might be (Ashraf *et al.*, 2021), pkC-SM web tool was used (<https://biosig.unimelb.edu.au/pkcsml/>) accessed on March 13, 2025.

Absorption: water solubility, Caco-2 permeability, P-glycoprotein interaction; Distribution: volume of distribution (Vd), BBB permeability; Metabolism: CYP450 enzyme interactions; Excretion: total clearance, OCT2 interaction; Toxicity: AMES test, hepatotoxicity, skin sensitization. the amount of the compound that remains free in the blood, and their ability to cross blood-brain barrier. Threshold criteria were defined according to (Pires *et al.*, 2015).

Statistical analysis

Data were analyzed using R software (v4.3.1). Results are expressed as mean ± SEM (3 independent replicates). Normality was assessed using the Shapiro–Wilk test, and homogeneity of variances using Levene’s test. Differences between groups were analyzed using one-way ANOVA. A P-value below 0.05 indicate a statistically significant difference.

RESULTS

Antimicrobial activity

Agar diffusion method

The antibacterial activity of the three extracts of *Cannabis sativa* L. leaf by-product were assessed using the agar well diffusion technique (Figure 7 and 8). Antimicrobial efficacy was quantified by measuring the diameters of growth inhibition zones surrounding the wells. The experimental findings are detailed in Table 1.

The one-way ANOVA test revealed a significant difference between the groups (p-value = 1.61e-07), highlighted by F(5, 12) = 47.96 in the treatment of *A. actinomycescomitans*, as well



Figure 7. Antifungal activity of *Cannabis sativa* L. leaf by-product extracts against *Candida albicans* ATCC 90028 by agar well diffusion method (E1: sonication; E2: maceration; E3: decoction; Chlr: chlorhexidine)



Figure 8. Antibacterial activity of *Cannabis sativa* L. leaf by-product extracts against *A. actinomycescomitans*

Table 1. Average diameters of inhibition zones (mm) generated by *Cannabis sativa* L. Leaf by-product extracts against the reference strains *A. actinomycescomitans* and *C. albicans*

Microbial strains studied	Diameters of inhibition zones (mm)						p _{value}
	Extracts			Solvents		Control +	
	Sonication	Maceration	Decoction	Distilled water	Hydro-ethanolique (20 :80)	Chlorexidine	
<i>A. actinomycescomitans</i> CCUG 56172	15.66 ± 1.53	13.16 ± 1.32	6 ± 0.00	6 ± 0.00	6 ± 0.00	24 ± 4	1.61 e ⁻⁰⁷
<i>C. albicans</i> ATCC 90028	12 ± 2.00	14 ± 0.00	6 ± 0.00	6 ± 0.00	6 ± 0.00	19.33 ± 3.05	3.7 e ⁻⁰⁷

Note: The diameter of the inhibition zone includes the diameter of the well (6 mm). All inhibition zone values are presented as mean ± SEM (mm).

as in the treatment of *Candida albicans* (p-value = 3.7e-07), with $F(5, 12) = 41.38$.

JP2 clone by agar well diffusion method (E1: sonication; E2: maceration; E3: decoction; T+: chlorhexidine)

Micro-dilution test

The MIC (Figure 9), MBC, and MFC (Figure 10) of the evaluated extracts were determined using the microdilution assay, the results are presented in Table 2.

Among the tested extracts, only those obtained by maceration and sonication exhibited effect against *A. actinomycetemcomitans*, with MIC values of 1 mg/mL and corresponding MBC values of 1.5 and 2 mg/mL, respectively. The MBC/MIC ratios (<4) confirmed a bactericidal effect. In contrast, the decoction extract showed no activity. Regarding antifungal activity, sonication (MIC = 8 mg/mL) was more effective than maceration (MIC = 9 mg/mL), while decoction remained inactive. Both active extracts presented identical MFC values (9 mg/mL), and MFC/MIC ratios <4, indicating fungicidal properties.

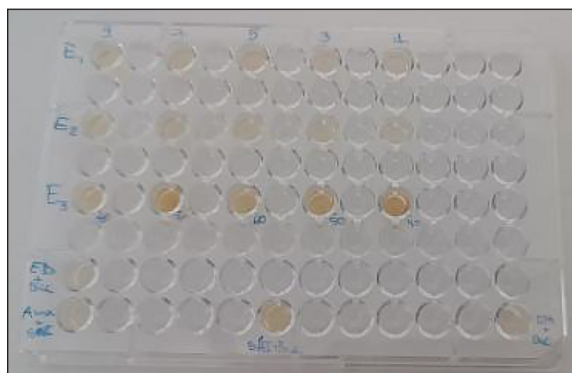


Figure 9. Determination of the Minimum Inhibitory Concentration (MIC) of *Cannabis sativa* L. leaf by-product extracts (E1: sonication; E2: maceration; E3: decoction) against *A. actinomycetemcomitans* JP2 clone by microdilution assay

Chemical composition

The phytochemical analysis of *Cannabis sativa* L. leaf co-products, obtained through sonication, maceration, and decoction as presented in Figure 11, revealed that cannabinoids represent the predominant class of metabolites, particularly in the sonication and maceration extracts. Alongside cannabinoids (e.g., cannabidiol, HU-331, cannabinol, and related derivatives), other classes such as flavonoids, phenols, alkaloids, lignans, and dihydrostilbenoids were also identified. In contrast, the decoction extract exhibited a much narrower profile, with only a few compounds (notably p-coumaric acid, hordenine, and cannabidiol) detected. All compounds, with their retention times and experimental masses, were confirmed by comparison with literature data, as summarized in Table 3.

In-silico analysis

Drug-likeness assessment of the chemical profile of *C. sativa*

In this study, the drug-likeness of 20 bioactive compounds derived from *Cannabis sativa* L. leaves was evaluated using the SWISS ADME tool, with particular reference to Lipinski’s Rule of Five (Table 4). Sixteen components fully complied with Lipinski’s criteria, suggesting promising absorption, distribution, and deliver properties. All logP values below five, designated compatibility with hydrophobic enzyme binding sites and acceptable pharmacokinetic behavior, allowing them for molecular docking studies. Inversely, four components (Caffeoyl-O-hexoside, Cannabisin A, Quercetin-O-sophoroside, and Chrysoeriol-O-glucuronide) didn’t respect all Lipinski’s rules and were rejected from subsequent analyses.

Molecular docking

Molecular docking was performed on 16 phytocompounds that complied with Lipinski’s

Table 2. MIC, MBC and MFC of *Cannabis sativa* L. Leaf By-product Extracts against the Periodontopathogen *A. actinomycetemcomitans* and the yeast *C. albicans*

Extracts	MIC (mg/ml)		MBC (mg/ml)	MFC (mg/ml)	MBC/MIC	MFC/MIC
	<i>A. actinomycetemcomitans</i>	<i>C. albicans</i>				
Sonication	1	8	2	9	2	1.125
Maceration	1	9	1.5	9	1.5	1
Decoction	-	-	-	-	-	-



Figure 10. Minimum bactericidal concentration of *Cannabis sativa* L. leaf by-product extracts against *A. actinomycetemcomitans* JP2 clone; sonication extract (E1, right) and maceration extract (E2, left)

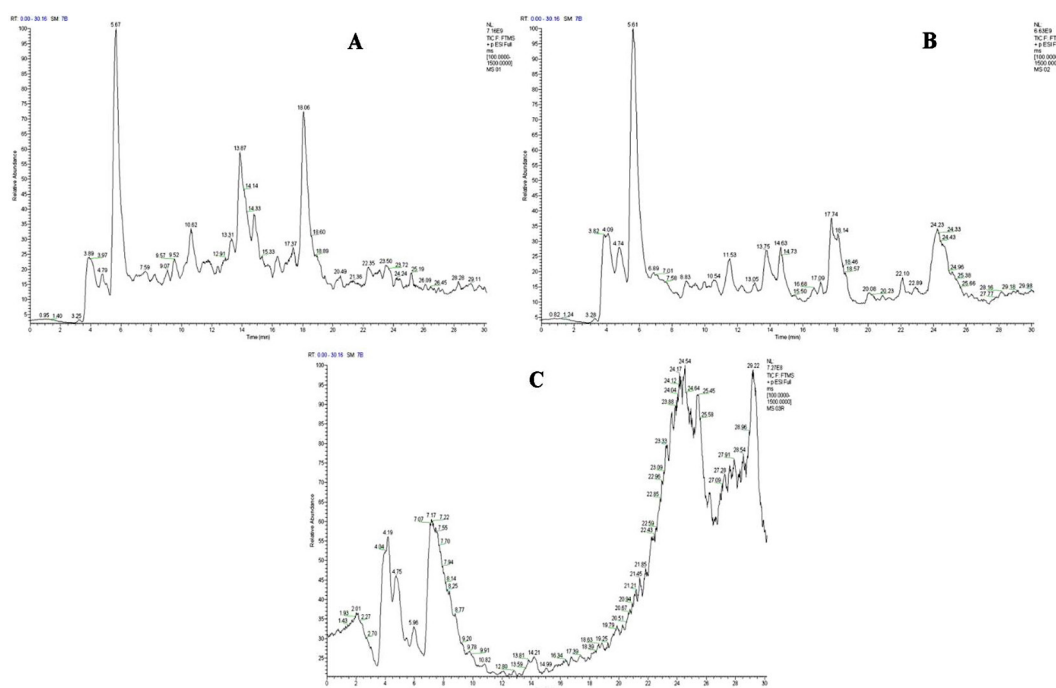


Figure 11. HPLC–MS chromatograms of *Cannabis sativa* L. leaves coproduct of sonication (A), maceration (B) and decoction (C) extracts

rules, targeting leukotoxin A (LtxA) and peptidyl arginine deiminase 4 (PAD4) (Table 5). Against LtxA, all compounds exhibited binding affinities comparable to or exceeding that of chlorhexidine (−6.9 kcal/mol) and interacted with the same key residues, though through diverse interaction types (hydrogen bonds, π -alkyl, π -sigma, van der Waals). Acacetin glycoside A showed the strongest affinity (−8.0 kcal/mol), forming hydrogen bonds with LYS259, ASN421, and ALA261, in addition to van der Waals interactions with LYS687 (Figure 12). For PAD4 (Figure 13), binding scores ranged from −4.9 to −8.4 kcal/mol, with all compounds engaging active site residues (Asp350, His471,

Asp473, Cys645). Acacetin glycoside A again displayed the highest affinity (−8.4 kcal/mol), forming hydrogen bonds with Cys645 and His471, while Cannflavin A (−7.6 kcal/mol) established multiple hydrogen bonds and a carbon–hydrogen bond with the catalytic residues.

In-silico pharmacokinetic (ADME) analysis

Pharmacokinetic and toxicity properties of the bioactive compounds were predicted in silico (Table 6). All components were water-soluble and exceeded the intestinal absorption threshold (>30%), with Cannabicyclic acid showing the

Table 3. List of compounds identified in the sonication, maceration, and decoction extracts of *Cannabis sativa* L. leaf co-products. Retention times and experimental masses were determined using atmospheric pressure chemical ionization (APCI)

Retention time			Compound name	Molecular formula	Theoretical mass	Experimental mass	References
Sonication	Maceration	Decoction					
		7.12, 7.53, 8.01,	p-Coumaric acid	C ₉ H ₈ O ₃	164.04	163	(Benkirane <i>et al.</i> , 2022)
		5.82	Hordenine	C ₁₀ H ₁₅ NO	166.1	166.1	(Pavlovic <i>et al.</i> , 2019)
12.39	12.15		Dihydroresveratrol	C ₁₄ H ₁₄ O ₃	231.1	231.1	(Pavlovic <i>et al.</i> , 2019)
	19.93, 20.87, 22.82		N-transcoumaroyltyramine		283.1	284	(Leonard <i>et al.</i> , 2021)
16.88, 17.07	16.63		Cannabinol	C ₂₁ H ₂₆ O ₂	310.2	311.2	(Moccia <i>et al.</i> , 2020)
9.07			N-feruloyltyramine	C ₁₈ H ₁₉ NO ₄	313.1	313	(Leonard <i>et al.</i> , 2021)
3.85	4.09		N-trans-feruloyltyramine	C ₁₈ H ₁₉ NO ₄	314.1	314.1	(Pavlovic <i>et al.</i> , 2019)
13.87, 18.06, 19.14, 20.20, 20.44	13.75, 18.19, 18.64	16.29	Cannabidiol	C ₂₁ H ₃₀ O ₂	315.1	315.2	(Brighenti <i>et al.</i> , 2017)
11.36, 12.02, 13.26, 17.22, 17.42	13.03, 17.11, 17.72		HU-331	C ₂₁ H ₂₈ O ₃	329.2	329.2	(Citti <i>et al.</i> , 2018)
16.31			Cannabigerovarinic acid	C ₂₁ H ₃₂ O ₃	333.2	333.2	(Pavlovic <i>et al.</i> , 2019)
14.82, 23.11, 25.17, 26.93	14.59		Caffeoyl-O-hexoside	C ₁₅ H ₁₈ O ₉	341	341.2	(Mazzara <i>et al.</i> , 2022)
28.23			Canniprene	C ₂₁ H ₂₆ O ₄	343.1	343.3	(Pavlovic <i>et al.</i> , 2019)
10.23			Cannabigerolic acid	C ₂₂ H ₃₂ O ₄	343.2	344.2	(Ferrer, 2020)
12.81			Cannabicyclic Acid	C ₂₀ H ₂₈ O ₄	345.2	345.2	(Pavlovic <i>et al.</i> , 2019)
10.65	10.49		Hydroxy-cannabidivarinic acid	C ₂₀ H ₂₆ O ₄	347	347.2	(Mazzara <i>et al.</i> , 2022)
9.52			Cannabiripsol	C ₂₁ H ₃₂ O ₄	349.2	349.2	(Pavlovic <i>et al.</i> , 2019)
22.30, 23.45	22.05		Cannabidiolic acid (CBDA)	C ₂₂ H ₃₀ O ₄	358.2	359.2	(Benkirane <i>et al.</i> , 2022)
11.68	11.50		Cannabielsoic acid	C ₂₂ H ₂₉ O ₅	374.2	373.2	(Benkirane <i>et al.</i> , 2022)
	26.64, 28.87, 29.16		Medioresinol	C ₂₁ H ₂₄ O ₇	388.1	388.4	(Moccia <i>et al.</i> , 2020)
	16.36		Cannflavin A	C ₂₆ H ₂₈ O ₆	437.2	437.2	(Pavlovic <i>et al.</i> , 2019)
29.04			Chrysoeriol-O-glucuronide	C ₂₂ H ₂₀ O ₁₂	477.1	477.3	(André <i>et al.</i> , 2020)
	3.80		Cannabisin A	C ₃₄ H ₃₀ N ₂ O ₈	594.2	595.2	(Benkirane <i>et al.</i> , 2022)
	28.11		Acacetin glycoside A	C ₂₂ H ₂₂ O ₁₀	623	621.3	(Mastellone <i>et al.</i> , 2022)
	25.98, 26.33, 26.90		Quercetin-O-sophoroside	C ₂₇ H ₃₀ O ₁₇	627.1	628.5	(André <i>et al.</i> , 2020)

highest HIA (98.2%). Skin permeability values indicated poor dermal absorption. Most compounds acted as P-gp substrates, with only a few functioning as inhibitors, suggesting favorable

oral bioavailability. Distribution analysis showed generally high volumes of distribution, with Cannabinol being the only compound predicted to cross the blood–brain barrier. Metabolic

Table 4. Molecular investigation of *C. sativa* phytochemicals for Drug-Likeness

Molecule	M. W (g/mol)	H. D	H. A	Log P _{ow}	Lipinski rule of five violation	Docking approval
Dihydroresveratrol	230.26	3	3	2.49	0	Yes
Cannabinol	310.43	1	2	5.21	1	Yes
N-feruloyltyramine	313.35	3	4	2.39	0	Yes
Cannabidiol	314.46	2	2	5.2	1	Yes
Cannabigerovarinic acid	332.43	3	4	4.65	0	Yes
Caffeoyl-O-hexoside	342.3	6	9	-0.92	2	No
Canniprene	342.43	2	4	4.32	0	Yes
Cannabigerolic acid	360.49	3	4	5.39	1	Yes
Hydroxy-cannabidivarinic acid	330.42	3	4	4.14	0	Yes
Cannabiripsol	348.48	3	4	3.65	0	Yes
N-transcoumaroyltyramine	283.32	3	3	2.46	0	Yes
Medioresinol	388.41	3	7	2.37	0	Yes
Cannflavin A	436.5	3	6	5.15	1	Yes
Cannabisin A	594.61	8	8	3.83	2	No
Acacetin glycoside A	446.40	5	10	0.9	0	Yes
Quercetin-O-sophoroside	626.52	11	17	-1.93	3	No
p-Coumaric acid	164.16	2	3	1.26	0	Yes
Hordenine	165.23	1	2	1.82	0	Yes
Cannabicyclic Acid	358.47	2	4	4.59	0	Yes
Chrysoeriol-O-glucuronide	476.39	6	12	0.32	2	No

Note: H. D – number of H donor; H. A – number of H acceptor.

predictions revealed limited CYP2D6 interaction, though several compounds displayed selective inhibition of other CYP isoforms. Renal clearance was moderate, and no compounds were substrates of OCT2 transporters. Toxicity predictions highlighted a generally safe profile, with only one compound showing AMES mutagenicity, three with potential hepatotoxicity, and six inhibiting hERG II but none hERG I, supporting an overall favorable cardiotoxicity profile.

DISCUSSION

Severe periodontal diseases affect over one billion people globally, with *A. actinomycetemcomitans* serotype b recognized as one of the most aggressive periodontopathogens, particularly in juveniles and adolescents (Gholizadeh *et al.*, 2017; WHO, 2025). *Candida albicans*, as an opportunistic fungal pathogen, further complicates the oral infectious landscape in immunocompromised individuals (Sardi *et al.*, 2010). The increasing resistance of both pathogens to conventional treatments underscores the need for novel, plant-derived alternatives.

The extraction method and solvent polarity substantially influenced the chemical composition and antimicrobial efficacy of the tested extracts, consistent with findings reported for other medicinal plants (Mohapatra *et al.*, 2021). Hydro-ethanolic sonication and maceration extracts yielded rich and diverse phytochemical profiles, while the aqueous decoction extract produced a markedly narrower profile and showed no detectable antimicrobial activity. This difference likely reflects the preferential solubility of the identified cannabinoids, stilbenoids, and flavonoids in polar organic solvents rather than water, though the precise contribution of individual compounds to the observed activity cannot be determined from the current data, as the extracts represent complex mixtures.

To our knowledge, this is the first study to assess the antimicrobial activity of *Cannabis sativa* L. leaf by-product extracts derived from mechanical processing waste specifically against *A. actinomycetemcomitans*. The only prior comparable work evaluated isolated cannabidiol (CBD) against this species, reporting MIC and MBC values of 1.56 µg/mL (Santos *et al.*, 2025). Our extracts, which are complex mixtures rather than pure compounds, showed MIC values of 1 mg/mL, reflecting the

Table 5. Binding affinity analysis of *C. sativa* leaves extracts potential ligands against two targets

Potential ligands	Binding score Kcal/mole		Interacting amino acid	
	LtxA	PAD4	LtxA	PAD4
Dihydroresveratrol	-6.1	-6.7	TRP478; ASN545; PHE450; ARG446; ASP479; THR474; GLN475; HIS447; GLN476; GLN480; TYR337	ASN588; ASP350; LEU410; GLU353; MET589; LEU590; GLU411; PHE407; GLY408; ARG651; ASN648; THR647
Cannabinol	-7.2	-7.6	ASN545; ASN1045; PHE450; PHE341; ARG446; THR474; GLN476; HIS447; GLN475	PHE407; ASP473; GLU411; CYS645; HIS471; VAL412; MET298; LEU410; GLU353; LEU590; MET589; THR647; ARG651; PRO300; ASN301
N-feruloyltyramine	-6.4	-7.5	TYR337; ASN1049; ALA1048; ASN1045; ALA449; PHE341; ASN545; GLN476; ARG446; ASP479; TRP478; GLN480	ARG651; LEU590; ILE630; VAL323; CYS645; ASN588; ASN301; SER322; GLY597; MET589; THR647; VAL649; VAL591
Cannabidiol	-6.5	-6.7	PHE341; ARG446; ALA449; PHE450; ASP479; TYR337; ARG340; GLN476; THR474; GLN475; SER454; LEU457; ASN545; LEU544	ASN588; THR647; VAL649; LEU590; CYS645; ILE630; GLY597; ASN648; ARG651; VAL323
Cannabigerovarinic acid	-6.9	-6.4	TYR337; ASP479; PHE450; PHE341; ARG446; ARG481; GLN480; GLN476; ASN545	ASP473; CYS645; THR647; HIS471; LEU590; GLU411; ARG651; VAL591; ASN648; VAL649; GLU353; PHE407
Canniprene	-6.7	-7	GLY477; ASN545; GLN476; PHE450; ALA1048; TYR337; ARG340; PHE341; ARG446; ARG481; ASP479	ASP350; CYS645; THR647; LEU590; VAL649; GLU353; ILE354; ASN648; GLY646; MET589; ARG651
Cannabigerolic acid	-6.4	-6.5	GLY477; ASN545; GLN476; PHE341; ARG446; PHE450; GLN475; LEU544; HIS447; TYR337; ARG481	THR647; HIS471; CYS645; ASP473; VAL649; ASN648; GLU411; ARG651; LEU590; VAL469; ASN588; GLU474
Hydroxy-cannabidivarinic acid	-6.7	-7	ARG481; ARG446; GLN480; ASP479; TYR337; TYR443; GLN476; PHE341; ARG340; TRP478	THR647; ASN588; CYS645; VAL649; LEU590; HIS471; PHE407; ASN648; GLU353; ARG651; VAL591; GLU411; ASP473
Cannabiripsol	-7.5	-7.7	TYR337; ASN1049; ALA1048; ARG446; PHE450; ASN545; THR474; HIS447; GLN476; TRP478; ASP479; GLN480	ASP473; THR647; VAL469; HIS471; VAL649; LEU590; GLY408; MET352; GLU353; PHE407; ASN648; LEU410; GLU411; MET589; ARG651; GLU474
N-transcoumaroyltyramine	-6.3	-6.9	ARG340; TYR337; ASN545; GLY477; ARG446; LEU544; PHE450; PHE341; GLN476	GLU353; LEU410; THR647; CYS645; HIS471; PHE407; GLY408; GLU411; VAL469; ASN648; ARG651
Medioresinol	-7.7	-7	ASN1049; PHE450; ASN545; TYR337; ALA1048; ASP479; HIS447; ARG446; GLN476; THR474; PHE341; ARG481	GLU411; ASP473; THR647; ASP632; ASN588; PRO599; ALA581; HIS471; ASN585; GLU474
Cannflavin A	-7.8	-7.6	ASN1041; ASN1045; PHE1044; PHE450; ARG446; ASN545; LEU544; THR474; GLN475; ALA449; GLN476; PHE341; ARG340	THR647; GLU411; ASP473; HIS471; CYS645; LEU590; ASN648; ASN301; ARG651; VAL591; ASP350
Acacetin glycoside A	-8	-8.4	LYS259; ASN421; ALA261; ARG490; ALA414; GLU417; ALA410; LYS687; TYR563; GLN413; HIS418; LYS266; THR263; ASP262; ASP260	CYS645; GLY408; HIS471; GLU353; ARG651; ASN301; MET589; VAL591; LEU590; GLU411; GLU474; VAL469; ASN648
p-Coumaric acid	-5.8	-5.5	ASN545; TYR337; ARG446; ASP479; PHE341; GLN476; PHE450; HIS447; GLN475; TYR501; THR474	VAL591; ASN301; ARG651; ASP473; MET589; LEU590; THR647; ASN648; ILE354; GLU353; MET352; PHE407; GLU411
Hordenine	-4.7	-4.9	ARG340; ARG446; PHE341; TYR337; TRP478; GLN480; ASP479; GLN476; PHE450; ALA449	ARG651; MET589; VAL591; LEU590; ASN301; VAL649; PHE407; ASP350; ASN548; GLU353; THR647; ASP473
Cannabicyclic Acid	-7.3	-7.5	PHE450; ARG446; ASN545; ASP453; SER454; ALA449; ARG340; PHE341; TYR337; ASP479; GLN476; GLN475	ASP473; GLU411; HIS471; LEU590; VAL649; VAL469; MET589; THR647; ARG651; ASN648; GLU353; GLY408
Chlorhexidine*	-6.9	--	ASN1045; PHE1044; PHE450; LEU544; GLN476; ASN545; ASP479; ARG446; TYR697; PRO546; ALA449; PHE341	--

Note: * Standard.

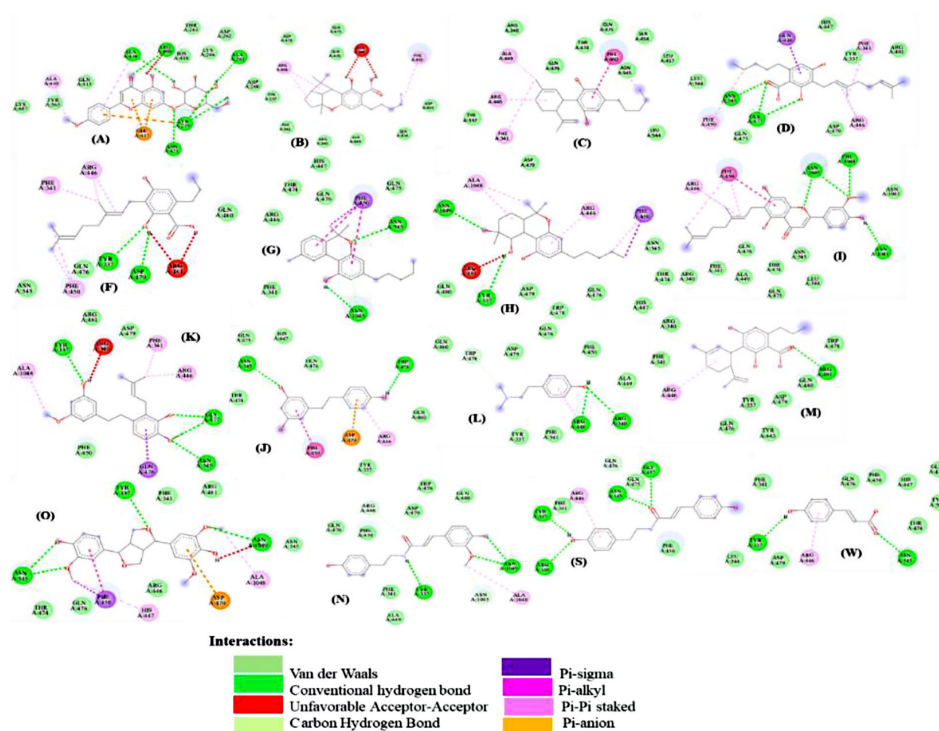


Figure 12. Visualization of the interaction between potential ligands from the hydroethanolic extract and the LtxA: A: Acacetin glycoside A; B: Cannabicyclic acid; C: Cannabidiol; D: Cannabigerolic acid; F: Cannabigerovarinic acid; G: Cannabinol; H: Cannabiripsol; I: Cannflavin A; K: Canniprene; J: Dihydroresveratrol; L: Hordenine; M: Hydroxy-cannabidivarinic acid; O: Medioresinol; N: N-feruloyltyramine; S: N-transcoumaroyltyramine; w: p-Coumaric acid

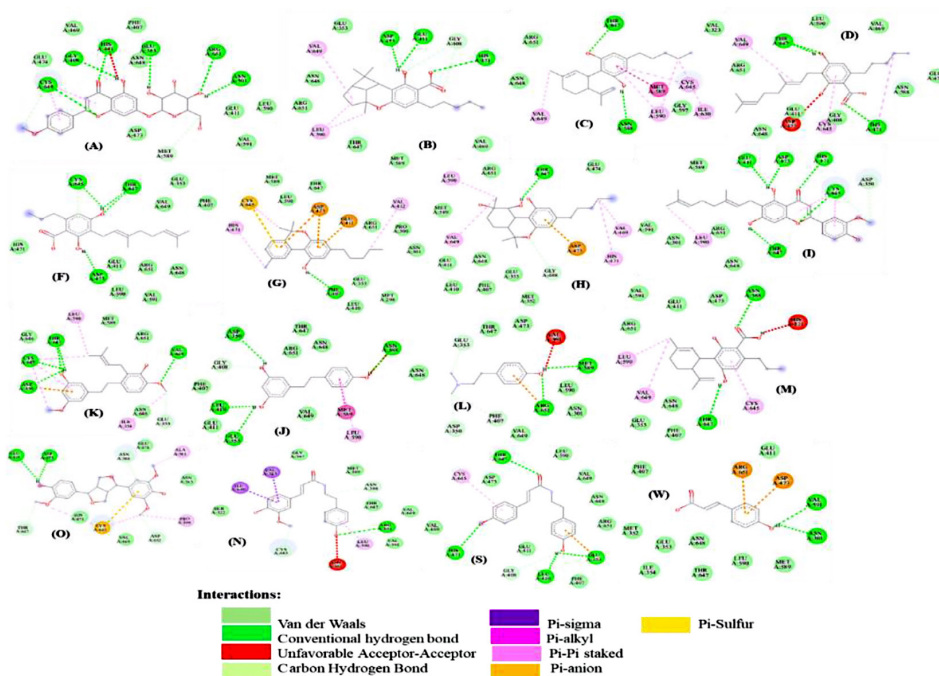


Figure 13. Visualization of the interaction between potential ligands from the hydroethanolic extract and the PAD4 enzyme: A: Acacetin glycoside A; B: Cannabicyclic acid; C: Cannabidiol; D: Cannabigerolic acid; F: Cannabigerovarinic acid; G: Cannabinol; H: Cannabiripsol; I: Cannflavin A; K: Canniprene; J: Dihydroresveratrol; L: Hordenine; M: Hydroxy-cannabidivarinic acid; O: Medioresinol; N: N-feruloyltyramine; S: N-transcoumaroyltyramine; w: p-Coumaric acid

Table 6. Pharmacokinetic prediction behavior of the potential ligands of hydroethanolic leaf

Parameter		Dihydroresveratrol	Cannabinol	N-feruloyltyramine	Cannabidiol	Cannabiger- ovarinic acid	Canniprene	Cannabigerolic acid	Hydroxy- cannabidivarinic acid
Absorption	Water solubility (log mol/L)	-3.142	-5.78	-3.292	-4.901	-3.094	-4.617	-3.224	-2.915
	Intestinal absorption %	91.819	92.487	90.23	90.657	94.644	91.466	93.963	95.841
	P-glycoprotein substrate	yes	yes	yes	yes	yes	yes	yes	Yes
	P-glycoprotein inhibitor	no	no	no	yes	no	yes	no	No
Distribution	VDss (log L/kg)	0.342	0.758	0.128	0.939	-1.661	0.169	-1.604	-1.474
	Fraction unbound (Fu)	0.187	0	0.045	0.012	0.056	0	0.003	0.143
	BBB permeability (log BB)	no	yes	no	no	no	no	no	No
	CNS permeability (log PS)	no	yes	no	yes	no	no	no	No
Metabolism	CYP2D6 substrate	no	no	no	no	no	no	no	No
	CYP3A4 substrate	yes	yes	yes	yes	no	yes	no	No
	CYP1A2 inhibitor	yes	yes	yes	yes	no	yes	no	no
	CYP2C19 inhibitor	yes	yes	yes	yes	no	yes	no	No
	CYP2C9 inhibitor	no	yes	no	no	no	yes	no	No
	CYP2D6 inhibitor	no	no	no	no	no	no	no	No
	CYP3A4 inhibitor	no	yes	yes	no	no	yes	no	No
Excretion	Total Clearance	0.115	0.777	0.27	1.092	1.099	0.324	1.165	0.878
	Renal OCT2 substrate	no	no	no	no	no	no	no	No
Toxicity	AMES toxicity	yes	no	no	no	no	no	no	No
	Max. tolerated dose (log mg/kg/day)	0.341	0.43	-0.106	0.324	0.306	0.273	0.202	0.467
	hERG I inhibitor	no	no	no	no	no	no	no	No
	hERG II inhibitor	no	yes	yes	yes	no	yes	no	No
	Hepatotoxicity	no	no	yes	no	no	no	no	Yes
	Skin Sensitisation	no	no	no	no	no	no	no	No
Parameter		Cannabiripsol	N-transcouma- royltyramine	Medioresinol	Cannflavin A	Acacetin glycoside A	p-Coumaric acid	Hordenine	Cannabicyclic acid
Absorption	Water solubility (log mol/L)	-4.511	-3.165	-3.453	-3.976	-3.029	-2.378	-1.219	-3.129
	Intestinal absorption %	93.036	90.031	91.403	89.429	46.529	93.494	93.396	98.218
	P-glycoprotein substrate	yes	yes	es	yes	yes	no	no	Yes
	P-glycoprotein inhibitor	yes	no	yes	yes	no	no	no	No
Distribution	VDss (log L/kg)	0.255	0.261	0.21	0.388	-0.312	-1.151	0.887	-1.212
	Fraction unbound (Fu)	0.072	0.149	0.021	0	0.138	0.428	0.549	0.084
	BBB permeability (log BB)	no	no	no	no	no	no	no	No
	CNS permeability (log PS)	no	no	no	no	no	no	yes	No
Metabolism	CYP2D6 substrate	no	no	no	no	no	no	yes	No
	CYP3A4 substrate	yes	yes	yes	yes	no	no	no	No
	CYP1A2 inhibitor	no	yes	no	yes	no	no	no	No
	CYP2C19 inhibitor	yes	yes	yes	yes	no	no	no	No
	CYP2C9 inhibitor	no	no	yes	yes	no	no	no	No
	CYP2D6 inhibitor	no	no	no	no	no	no	no	No
	CYP3A4 inhibitor	no	no	yes	yes	no	no	no	No
Excretion	Total Clearance	0.73	0.265	0.05	0.42	0.644	0.662	0.907	0.449
	Renal OCT2 substrate	no	no	no	no	no	no	yes	No

expected difference in potency between isolated molecules and crude extracts. It is important to note that direct numerical comparisons with values reported in other studies are not meaningful, given the substantial differences in strains, solvents, extract concentrations, and experimental protocols employed across the literature (Obaid *et al.*, 2022; Serventi *et al.*, 2023; Haddou *et al.*, 2023).

Cannabidiol was the most frequently detected compound across the active extracts, alongside HU-331, cannabinol, stilbenoids, lignans, flavonoids, and alkaloids. The presence of these compound classes in *Cannabis sativa* leaves is consistent with previously reported phytochemical profiles (Judžentienė *et al.*, 2023; De Vita *et al.*, 2022; Guo *et al.*, 2018). However, attributing the observed antimicrobial activity to any single compound would be premature without further fractionation and bioassay-guided isolation studies.

The drug-likeness assessment revealed that 16 of the 20 identified compounds complied with Lipinski's Rule of Five, indicating potentially acceptable oral bioavailability. Notably, four compounds — Caffeoyl-O-hexoside, Cannabisin A, Quercetin-O-sophoroside, and Chrysoeriol-O-glucuronide — violated multiple criteria and were excluded from subsequent docking analyses. Among the remaining compounds, Acacetin glycoside A showed the lowest intestinal absorption (46.5%), which may limit its oral bioavailability despite satisfying Lipinski's criteria, while Cannabicyclic acid displayed the highest predicted intestinal absorption (98.2%). These compound-specific observations are relevant when prioritizing candidates for further development.

Molecular docking simulations suggested that several identified compounds may interact favorably with two virulence-associated targets: leukotoxin A (LtxA), a key mediator of *A. actinomycescomitans* pathogenicity, and peptidyl arginine deiminase 4 (PAD4), implicated in periodontal inflammation. All 16 docked compounds exhibited predicted binding affinities against LtxA ranging from -4.7 to -8.0 kcal/mol, with Acacetin glycoside A (-8.0 kcal/mol) and Cannflavin A (-7.8 kcal/mol) showing the most favorable scores, exceeding that of chlorhexidine (-6.9 kcal/mol). Against PAD4, binding scores ranged from -4.9 to -8.4 kcal/mol, again with Acacetin glycoside A displaying the highest affinity. These results suggest potential inhibitory interactions worthy of further investigation. It must be emphasized, however, that docking is a computational

prediction tool and does not constitute experimental evidence of inhibition. The predicted interactions remain to be validated through enzymatic assays and cell-based studies. Furthermore, the LtxA structure used in this study is an AlphaFold-predicted model, as no experimentally resolved crystal structure is currently available, which introduces an additional layer of uncertainty in the interpretation of docking results.

In silico ADME and toxicity predictions indicated that the majority of identified compounds have generally favorable pharmacokinetic profiles, with acceptable water solubility, high intestinal absorption, and a low toxicity burden only one compound showed AMES mutagenicity, and three showed predicted hepatotoxicity. While these predictions are encouraging, they are inherently limited by the computational nature of the tools employed and should be regarded as hypothesis-generating rather than conclusive.

Several limitations of the current study should be acknowledged. First, the antimicrobial activity was assessed using crude extracts, making it impossible to attribute observed effects to specific compounds without bioassay-guided fractionation. Second, all biological activity data were generated *in vitro*, and the relevance of these findings to *in vivo* conditions remains to be established. Third, the docking simulations do not account for protein flexibility, solvent effects, or physiological binding conditions. Finally, the study was conducted on reference strains only; clinical isolates with varying resistance profiles may respond differently.

CONCLUSIONS

The aim of this study was fully achieved. Sonication and maceration extracts of *Cannabis sativa* L. leaf by-products demonstrated significant antimicrobial activity against *A. actinomycescomitans* and *C. albicans*, with confirmed bactericidal and fungicidal effects, thereby supporting H1. The marked difference in activity between hydro-ethanolic and aqueous extracts confirmed H2, as extraction method and solvent polarity critically determined both chemical composition and biological efficacy. H3 was likewise supported, with *in silico* docking revealing that 16 identified compounds exhibited binding affinities against LtxA and PAD4 comparable to or exceeding that of chlorhexidine, and ADME analysis indicating a generally favorable pharmacokinetic profile.

The principal novel contribution of this study lies in being the first to evaluate whole *Cannabis sativa* L. leaf by-product extracts against the periodontopathogen *A. actinomycetemcomitans* JP2 clone, filling a documented gap in the literature regarding both the antimicrobial valorization of this underutilized agricultural waste and the mechanistic understanding of its bioactive compounds. These findings open perspectives for the development of plant-derived oral antimicrobial agents, and future work should focus on the isolation of the most active compounds, in vivo validation, and their integration into oral healthcare formulations.

REFERENCES

1. Abdallah, E. M., Alhatlani, B. Y., De Paula Menezes, R., Martins, C. H. G. (2023). Back to nature: Medicinal plants as promising sources for antibacterial drugs in the post-antibiotic era. *Plants* 12(17), 3077. <https://doi.org/10.3390/plants12173077>
2. Alsina, M., Olle, E., Frias, J. (2001). Improved, low-cost selective culture medium for *Actinobacillus Actinomycetemcomitans*. *Journal of Clinical Microbiology* 39(2), 509–13. <https://doi.org/10.1128/JCM.39.2.509-513.2001>
3. André, A., Leupin, M., Kneubühl, M., Pedan, V., Chetschik, I. (2020). Evolution of the polyphenol and terpene content, antioxidant activity and plant morphology of eight different fiber-type cultivars of *Cannabis Sativa* L. cultivated at three sowing densities. *Plants* 9(12), 1740. <https://doi.org/10.3390/plants9121740>
4. Ashraf, S. A., Elkhalfifa, A. E. O., Mehmood, K., Adnan, M., Khan, M. A., Eltoun, N. E., Krishnan, A., Baig, M. S. (2021). Multi-targeted molecular docking, pharmacokinetics, and drug-likeness evaluation of okra-derived ligand abscisic acid targeting signaling proteins involved in the development of diabetes. *Molecules* 26(19), 5957.
5. Benkirane, C., Ben Moumen, A., Fauconnier, M. L., Belhaj, K., Abid, M., Caid, H. S., Elamrani, A., Mansouri, F. (2022). Bioactive Compounds from Hemp (*Cannabis Sativa* L.) Seeds: Optimization of phenolic antioxidant extraction using simplex lattice mixture design and HPLC-DAD/ESI-MS 2 analysis. *RSC Advances* 12(39), 25764-77. <https://doi.org/10.1039/D2RA04081F>
6. Bonini, S. A., Premoli, M., Tambaro, S., Kumar, A., Maccarinelli, G., Memo, M., Mastinu, A. (2018). *Cannabis sativa*: A comprehensive ethnopharmacological review of a medicinal plant with a long history. *Journal of Ethnopharmacology* 227, 300–315. <https://doi.org/10.1016/j.jep.2018.09.004>
7. Brighenti, V., Pellati, F., Steinbach, M., Maran, D., Benvenuti, S. (2017). Development of a new extraction technique and HPLC method for the analysis of non-psychoactive cannabinoids in fibre-type *Cannabis sativa* L. (Hemp). *Journal of Pharmaceutical and Biomedical Analysis* 143, 228–36. <https://doi.org/10.1016/j.jpba.2017.05.049>
8. Citti, C., Battisti, U. M., Braghiroli, D., Ciccarella, G., Schmid, M., Vandelli, M. A., Cannazza, G. (2018). A metabolomic approach applied to a liquid chromatography coupled to high-resolution tandem mass spectrometry method (HPLC-ESI-HRMS/MS): Towards the comprehensive evaluation of the chemical composition of cannabis medicinal extracts. *Phytochemical Analysis* 29(2), 144–55. <https://doi.org/10.1002/pca.2722>
9. Cockerill F. R., Clinical and Laboratory Standards Institute. (2012) Methods for Dilution Antimicrobial Susceptibility Tests for Bacteria That Grow Aerobically: Approved Standard - Ninth Edition. *Clinical and Laboratory Standards Institute M07-A9 = 32.2*. CLSI.
10. De Vita, S., Finamore, C., Chini, M. G., Saviano, G., De Felice, V., De Marino, S., Lauro, G., Casapullo, A., Fantasma, F., Trombetta, F., Bifulco, G., Lorizzi, M. (2022). Phytochemical analysis of the methanolic extract and essential oil from leaves of industrial hemp Futura 75 cultivar: isolation of a new cannabinoid derivative and biological profile using computational approaches. *Plants* 11(13), 1671. <https://doi.org/10.3390/plants11131671>
11. El-Mernissi, R., El Menyiy, N., Moubachir, R., Zouhri, A., El-Mernissi, Y., Siddique, F., Nadeem, S., Ibork, H., El Barnossi, A., Wondmie, G. F., Bourhia, M., Bin Jardan, Y. A., Aboussi, O., Hajji, L. (2024). *Cannabis sativa* L. Essential oil: Chemical composition, anti-oxidant, anti-microbial properties, and acute toxicity: In vitro, in vivo, and in silico study. *Open Chemistry* 22(1). <https://doi.org/10.1515/chem-2023-0214>
12. Ferrer, I. (2020). Analyses of Cannabinoids in Hemp Oils by LC/Q-TOF-MS In Comprehensive Analytical Chemistry 90, 415–52. Elsevier. <https://doi.org/10.1016/bs.coac.2020.04.014>
13. Gholizadeh, P., Pormohammad, A., Eslami, H., Shokouhi, B., Fakhrzadeh, V., Kafil, H. S. (2017). Oral pathogenesis of *Aggregatibacter actinomycetemcomitans*. *Microbial Pathogenesis* 113, 303–11. <https://doi.org/10.1016/j.micpath.2017.11.001>
14. Guo T, Liu Q, Hou P, Li F, Guo S, Song W, Zhang, H., Liu, X., Zhang, S., Zhang, J., Ho, C. T., Bai, N. (2018). Stilbenoids and cannabinoids from the leaves of *Cannabis sativa* f. *sativa* with potential reverse cholesterol transport activity. *Food & function* 9(12), 6608–6617. <https://doi.org/10.1039/c8fo01896k>

15. Haddou, S., Mounime, K., Loukili, E., Ou-Yahia, D., Hbika, A., Idrissi, M. Y., Legssyer, A., Lgaz, H., Asehrou, A., Touzani, R., Hamouti, B., Chahine, A. (2023). Investigating the biological activities of Moroccan *Cannabis sativa* L seed extracts: Antimicrobial, anti-inflammatory, and antioxidant effects with molecular docking analysis. *Moroccan Journal of Chemistry* 11(4), 1116–1136. <https://doi.org/10.48317/IMIST.PRSM/MORJCHEM-V11I04.42100>
16. Jamshidi-Kia, F., Lorigooini, Z., Amini-Khoei, H. (2017). Medicinal plants: Past history and future perspective. *Journal of Herbmmed Pharmacology* 7(1), 1–7. <https://doi.org/10.15171/jhp.2018.01>
17. Judžentienė, A., Garjonytė, R., Būdienė, J. (2023). Phytochemical composition and antioxidant activity of various extracts of fibre hemp (*Cannabis sativa* L.) cultivated in Lithuania. *Molecules* 28(13), 4928. <https://doi.org/10.3390/molecules28134928>
18. Kebede, T., Gadisa, E., Tufa, A. (2021). Antimicrobial activities evaluation and phytochemical screening of some selected medicinal plants: A possible alternative in the treatment of multidrug-resistant microbes. *PLOS ONE* 16(3), e0249253. <https://doi.org/10.1371/journal.pone.0249253>
19. Khalandi, H., Masoori, L., Farahyar, S., Delbandi, A. A., Raiesi, O., Farzanegan, A., Khalandi, G., Mahmoudi, S., Erfanirad, T., Falahati, M. (2020). Antifungal activity of capric acid, nystatin, and flucanazole and their *In Vitro* interactions against *Candida* Isolates from neonatal oral thrush. *ASSAY and Drug Development Technologies* 18(4), 195–201. <https://doi.org/10.1089/adt.2020.971>
20. Leonard, W., Zhang, P., Ying, D., Xiong, Y., Fang, Z. (2021). Extrusion improves the phenolic profile and biological activities of hempseed (*Cannabis Sativa* L.) hull. *Food Chemistry* 346, 128606. <https://doi.org/10.1016/j.foodchem.2020.128606>
21. Lipinski, C. A., Lombardo, F., Dominy, B. W., Feeney, P. J. (2012). Experimental and computational approaches to estimate solubility and permeability in drug discovery and development settings. *Advanced Drug Delivery Reviews* 64,4–17. <https://doi.org/10.1016/j.addr.2012.09.019>
22. Mastellone, G., Marengo, A., Sgorbini, B., Scaglia, F., Capetti, F., Gai, F. (2022). Characterization and biological activity of fiber-type *Cannabis sativa* L. aerial parts at different growth stages. *Plants* 11(3), 419. <https://doi.org/10.3390/plants11030419>
23. Mazzara, E., Carletti, R., Petrelli, R., Mustafa, A. M., Caprioli, G., Fiorini, D. (2022). Green extraction of hemp (*Cannabis sativa* L.) using microwave method for recovery of three valuable fractions (essential oil, phenolic compounds and cannabinoids): A central composite design optimization study. *Journal of the Science of Food and Agriculture* 102(14), 6220–35. <https://doi.org/10.1002/jsfa.11971>
24. Moccia, S., Siano, F., Russo, G. L., Volpe, M. G., La Cara, F., Pacifico, S., Piccolella, S., Picariello, G. (2020). Antiproliferative and antioxidant effect of polar hemp extracts (*Cannabis sativa* L., Fedora Cv.) in human colorectal cell lines. *International Journal of Food Sciences and Nutrition* 71(4), 410–23. <https://doi.org/10.1080/09637486.2019.1666804>
25. Mohapatra, P., Ray, A., Jena, S., Nayak, S., Mohanty, S. (2021). Influence of extraction methods and solvent system on the chemical composition and antioxidant activity of *Centella Asiatica* L. Leaves. *Biocatalysis and Agricultural Biotechnology* 33,101971. <https://doi.org/10.1016/j.bcab.2021.101971>
26. Obaid, R. F., Hindi, N. K. K., Kadhum, S. A., Alwaeli, L. A., Jalil, A. T. (2022). Antibacterial activity anti-adherence and anti-biofilm activities of plants extracts against *Aggregatibacter actinomycetemcomitans*: An in vitro study in Hilla City Iraq. *Caspian Journal of Environmental Sciences* 20(2). <https://doi.org/10.22124/cjes.2022.5578>
27. Odds, F. C. (1991). Sabouraud('s) Agar. *Medical Mycology* 29(6), 355–59. <https://doi.org/10.1080/02681219180000581>
28. Pavlovic, R., Panseri, S., Giupponi, L., Leoni, V., Citti, C., Cattaneo, C., Cavaletto, M., Giorgi, A. (2019). Phytochemical and ecological analysis of two varieties of hemp (*Cannabis Sativa* L.) grown in a mountain environment of Italian Alps. *Frontiers in Plant Science* 10. <https://doi.org/10.3389/fpls.2019.01265>
29. Pires, D. E., Blundell, T. L., Ascher, D. B. (2015). pkCSM: predicting small-molecule pharmacokinetic and toxicity properties using graph-based signatures. *Journal of medicinal chemistry* 58(9), 4066–4072.
30. Raeber, J., Poetzsch, M., Shmidli, A., Favrod, S., Steuer, C. (2024). Simultaneous quantification of terpenes and cannabinoids by reversed-phase LC-APCI-MS/MS in *Cannabis sativa* L. samples combined with a subsequent chemometric analysis. *Analytical and Bioanalytical Chemistry* 416(18), 4193–4206. <https://doi.org/10.1007/s00216-024-05349-y>
31. Rather, M. A., Gupta, K., Bardhan, P., Borah, M., Sarkar, A., Eldiehy, K. S. H., Bhuyan, S., Mandal, M. (2021). Microbial biofilm: A matter of grave concern for human health and food industry. *Journal of Basic Microbiology* 61(5), 380–95. <https://doi.org/10.1002/jobm.202000678>
32. Santos, A. L. O., Santiago, M. B., Silva, N. B. S., Souza, S. L., Almeida, J. M. D., Martins, C. H. G. (2025). The antibacterial and antibiofilm role of cannabidiol against periodontopathogenic bacteria. *Journal of Applied Microbiology* 136(1), lxae316. <https://doi.org/10.1093/jambio/lxae316>

